Toxicology and Applied Pharmacology **178,** 117–125 (2002)
doi:10.1006/taap.2001.9267, available online at http://www.idealibrary.com on IDEAL®

p21$^{WAF1/CIP1}$ Inhibits Cell Cycle Progression but Not G2/M-Phase Transition Following Methylmercury Exposure

Ma Aileen C. Mendoza,* Rafael A. Ponce,*,† Ying C. Ou,‡ and Elaine M. Faustman*,†,§,[1]

*Department of Environmental Health, University of Washington, Seattle, Washington 98195; †Center for Ecogenetics and Environmental Health and Institute for Risk Analysis and Risk Communication, Seattle, Washington 98195; ‡Center for Environmental Toxicology and Technology, Colorado State University, Fort Collins, Colorado 80523; and §Center on Human Development and Disability, Seattle, Washington 98195

Received March 1, 2001; accepted July 1, 2001

p21$^{WAF1/CIP1}$ Inhibits Cell Cycle Progression but Not G2/M-Phase Transition Following Methylmercury Exposure. Mendoza, M. A. C., Ponce, R. A., Ou, Y. C., and Faustman, E. M. (2002). *Toxicol. Appl. Pharmacol.* **178, 117–125.**

Methylmercury (MeHg) is an environmentally prevalent organometal that is particularly toxic to the developing central nervous system (CNS). Prenatal MeHg exposure is associated with reduced brain size and weight and a reduced number of neurons, which have been associated with impaired cell proliferation. We evaluate the role of p21, a cell cycle protein involved in the G_1- and G_2-phase checkpoint control, in the cell cycle inhibition induced by MeHg. Primary mouse embryonic fibroblasts (MEFs) of different p21 genotypes (wild-type, heterozygous, and null) were isolated at day 14 of gestation and treated at passages 4–6 with either 0, 2, 4, or 6 μM MeHg or 50 nM colchicine for 24 h. Changes in cell cycle distribution after continuous toxicant treatment were analyzed by DNA content-based flow cytometry using DAPI. MeHg induced an increase in the proportion of cells in G_2/M at 2 and 4 μM MeHg ($p \leq 0.05$) irrespective of p21 genotype. Effects of MeHg on cell cycle progression were subsequently evaluated using BrdU–Hoechst flow cytometric analysis. Inhibition of cell cycle progression was observed in all p21 genotypes after continuous exposure to MeHg for 24 and 48 h. p21 null (−/−) cells reached the second-round G_1 at a higher fraction compared to the wild type (+/+) and heterozygous (+/−) cells ($p \leq 0.05$). These data support previous observations that MeHg inhibits cell cycle progression through delayed G_2/M transition. Whereas the G_2/M accumulation induced by MeHg was independent of p21 status, a greater proportion of p21(−/−) cells were able to complete one round of cell division in the presence of MeHg compared to p21(+/−) or p21(+/+) cells. These data suggest a role for p21 in retarding cell cycle progression, but not mitotic inhibition, following exposure to MeHg. © 2002 Elsevier Science (USA)

Key Words: **methylmercury; p21$^{WAF1;\ CIP1}$; cell cycle.**

Public health concern about exposures to environmental mercury has been heightened by the recognized toxicity of its organic form, methylmercury (MeHg)[2]. Epidemiological studies of outbreaks in Japan and Iraq and toxicological studies in rodents, nonhuman primates, and other species, have linked MeHg exposure to central nervous system (CNS) toxicity. Pathological examination of MeHg-exposed brains revealed localized lesions in adults as opposed to a diffuse pattern of injury following prenatal exposure (Takeuchi, 1968). Characteristic neuropathological findings following prenatal MeHg exposure include reduced cell number, disorganization of the cortical cytoarchitecture, hypoplasia of the granular layer in the cerebellum, and reduction in brain weight in both humans and experimentally exposed animals (Choi, 1986, 1989; Choi *et al.*, 1978; Eto *et al.*, 1992; Geelen *et al.*, 1990; Matsumoto *et al.*, 1965; Mottet, 1989; Takeuchi, 1977). Concentration and duration of exposure may not be sufficient to explain the sensitivity of the developing nervous system to MeHg toxicity, as mothers of affected fetuses may be asymptomatic (Harada, 1977, 1978; Marsh *et al.*, 1980; Takeuchi, 1977). Normal CNS development involves synchronization between cell proliferation, migration, differentiation, and selective loss in order to form the ordered connections characterizing the mature CNS (Herschkowitz, 1988). Disturbance of the timing of molecular signaling or effects on specific molecules involved in regulating cell behavior may be ways by which environmental insults perturb normal CNS development, and these effects may explain both the relative sensitivity of the fetus to MeHg toxicity and the neuropathological differences between the fetal and adult forms of Minamata disease (Levitt *et al.*, 1998; Rodier *et al.*, 1996). These observations support the possibility that the microcephaly and reduced cell number observed following prenatal MeHg exposure result from alterations in cell cycle regulatory processes.

Several investigators have found reduced numbers of cells in

[1] To whom correspondence should be addressed at the Department of Environmental Health, 4225 Roosevelt Way NE, Suite 100, University of Washington, Seattle, WA 98105. Fax: (206) 685-4696; E-mail: faustman@u.washington.edu.

[2] Abbreviations used: BrdU, 5-bromo-2′-deoxyuridine; CDK, cyclin-dependent kinase; CNS, central nervous system; DAPI, 4,6-diamidino-2-phenylindole; EB, ethidium bromide; G_1, gap 1 phase of cell cycle; G_2, gap 2 phase of cell cycle; LDH, lactate dehydrogenase; M, mitosis; MEFs: mouse embryonic fibroblasts; MeHg, methylmercury; PCNA, proliferating cell nuclear antigen; S, DNA synthesis phase of cell cycle.

0041-008X/02 $35.00

the cerebellum of rodents exposed to MeHg *in utero* without observed necrosis or alteration in protein synthesis. These findings suggest that the observed reduction in cell number is due to decreased cell production rather than cell loss (Howard and Mottet, 1986; Mottet, 1989; Sager *et al.*, 1984). Cell cycle inhibition, particularly in G_2/M, has been observed in MeHg-exposed cells *in vitro* (Ponce *et al.*, 1994; Vogel *et al.*, 1986), consistent with an increase in mitotic figures observed in gestationally exposed animals (Rodier *et al.*, 1984). We have previously observed $p21^{WAF1/CIP1}$ induction after MeHg treatment of primary fetal rat CNS cells (Ou *et al.*, 1999) under conditions leading to cell cycle inhibition (Ponce *et al.*, 1994). The mechanisms underlying altered cell cycling induced by MeHg remain incompletely understood.

The cell cycle is regulated by a number of proteins, including the cyclin-dependent kinase inhibitor $p21^{WAF1/CIP1}$. $p21^{WAF1/CIP1}$ is a component of the G_1 checkpoint (Brugarolas *et al.*, 1999; Cox, 1997; Cox and Lane, 1995) and may regulate G_2 to M phase transition (Bunz *et al.*, 1998; Niculescu *et al.*, 1998; Rigberg *et al.*, 1999). $p21^{WAF1/CIP1}$ inhibits cell cycle progression by binding to regulatory complexes, including cyclin E- cyclin-dependent kinase (CDK)2, which controls G_1 to S phase transition (Stewart *et al.*, 1999), cyclin B1-cdc2, which regulates progression from G_2 into mitosis (Barboule *et al.*, 1999; Dulic *et al.*, 1998), and PCNA, which results in both G_1 and G_2 arrest (Cayrol *et al.*, 1998). In the present study, we examined the effects of MeHg exposure on the cellular proliferation of primary embryonic fibroblasts of different p21 genotypes: wild-type (+/+), heterozygous (+/−), and null (−/−).

METHODS

Cell culture. The p21 transgenic mice backcrossed to the NIH strain (white) from the 129 × black Swiss hybrids originally bred by Dr. Phil Leder (Harvard Medical School, Boston, MA) were generously provided by Dr. Matthew Fero and Dr. Chris Kemp (Fred Hutchinson Cancer Research Center, Seattle, WA). Primary embryonic fibroblasts were prepared according to Robertson *et al.* (1987) with some modifications. Briefly, gravid uteri were removed from pregnant mice 14 days after a successful heterozygote cross. The embryos were isolated and washed separately several times in Earl's Balanced Salt Solution (Gibco BRL, Grand Island, NY). Fibroblasts were obtained from the torso and limbs. Tail DNA was used for genotyping by polymerase chain reaction using primers specific for the p21 wild-type allele and the mutated allele containing a *neo* cassette insert, which deletes exon 2 of the $p21^{WAF1/CIP1}$ gene (Deng *et al.*, 1995). Tissue dissociation was performed using 0.25% (w/v) trypsin (DIFCO, Detroit, MI), overnight at 4°C. Single-cell suspensions were obtained the next day and plated in 100-mm tissue culture dishes (Corning, Corning, NY). Cultures were maintained in Dulbecco's modified Eagle's medium (DMEM, Gibco BRL) containing 10% (v/v) fetal bovine serum (FBS, Gibco BRL), 200 units/ml penicillin (Sigma, St. Louis, MO), and 0.1 mg/ml streptomycin (Sigma) at 37°C in humidified air containing 5% CO_2. Cells were cultured until passage 3–4 and then plated in 60-mm tissue culture dishes (Corning). Cell density was adjusted to obtain uniform confluence prior to treatment. Culture stocks were stored at −80°C in DMEM containing 20% (v/v) FBS and 10% (v/v) dimethyl sulfoxide (DMSO, Sigma).

MeHg treatment. Working solutions giving final concentrations of 2, 4, and 6 μM MeHg were prepared from 10^3-fold dilution of a 1 M methylmercury(II) hydroxide stock solution (Alfa Aesar, Ward Hill, MA) using sterile water (Baxter, Deerfield, IL). Subconfluent cells (passages 4–6) grown overnight in 60-mm dishes were used for treatment. Sterile water was used as negative control while 50 nM colchicine (Sigma), a known G_2/M inhibitor, was used as positive control. For BrdU–Hoechst analysis, 5-bromo-2′-deoxyuridine (BrdU, Sigma), a nucleotide analog that is substituted for thymidine during DNA synthesis, was added to cultures at a final concentration of 90 μM. The treated plates were placed in a light-tight Plexiglas chamber containing water to maintain humidity, purged with 5% CO_2/95% air for 10 min, and incubated at 37°C for 24 to 48 h (Ponce *et al.*, 1994). Treatment was conducted in minimal light in a Class II Type B2 hood (Biochemguard, Baker Co., Sanford, ME).

Flow cytometry. After incubation, the MeHg-containing culture media was removed and the culture dishes were washed with calcium- and magnesium-free phosphate-buffered saline (CMF—PBS, pH 7.2, Gibco BRL) to rid cells of residual MeHg. Cells were harvested using 0.05% (w/v) trypsin in CMF–PBS containing 0.02% (w/v) EDTA (Fisher Scientific, Fair Lawn, NJ). The cell pellet was then resuspended in either 400 μl of 10 μg/ml 4,6-diamidino-2-phenylindole (DAPI, Sigma) containing 10% (v/v) DMSO or 400 μl of 1.2 μg/ml Hoechst 33258 (Molecular Probes Inc., Eugene, OR) containing 10% (v/v) DMSO and 0.1% (v/v) Nonidet-P40 (Sigma) and gradually frozen to −20°C until analysis.

DNA content analysis using DAPI was performed as previously described (Reid *et al.*, 1987, 1992) with some modifications. Briefly, thawed cells were forced through a 25–5/8 gauge syringe needle (Becton-Dickinson and Co., Franklin Lakes, NJ) several times and then passed through a 40-μm wire mesh filter (Small Parts, Miami Lakes, FL) to disaggregrate cells and to minimize clumps. Flow cytometry was performed on a Coulter Epics Elite flow cytometer (Coulter Corporation, Miami, FL). Relative DNA content per cell was estimated by measuring the fluorescence of DAPI, a blue fluorescent dye that binds stoichiometrically to DNA. A 20-mW UV laser (Innova 90–6, Coherent, Palo Alto, CA) emitting 335 nm ultraviolet light and a 450/35 nm band pass filter were used to excite and collect DAPI fluorescence. The flow rate was maintained at less than 300 cells per second and the data were collected and stored using Coulter Elite software version 4.01 (Coulter Corporation). A minimum of 10,000 events per sample were analyzed. Clumps and doublets were excluded from analysis by electronic gating, and the cell cycle distribution was quantified using MPLUS software (Phoenix Flow Systems, San Diego, CA).

BrdU–Hoechst analysis was performed according to established procedures (Rabinovitch, 1983, 1988). Fibroblasts were thawed and a 4 μg/ml final concentration of ethidium bromide (EB, Sigma), a red fluorescent dye that intercalates stoichiometrically in DNA, was added. Cells were then forced through a 25–5/8 gauge syringe needle several times and then passed through a 40-μm wire mesh filter to eliminate clumps. Flow cytometry was performed in a Coulter Epics Elite flow cytometer using a UV laser emitting 335 nm ultraviolet light. A 450/35 nm band pass filter was used to collect the Hoechst 33258 fluorescence. Hoechst 33258 binds to AT-rich regions in DNA and its fluorescence is proportionally quenched as cycling cells incorporate BrdU (Bohmer, 1979; Bohmer and Ellwart, 1981; Poot *et al.*, 1990; Rabinovitch *et al.*, 1988). An air-cooled 15 mW argon ion laser (Cyonics, San Jose, CA) emitting 488 nm light was used with a 590 nm long pass filter to excite and collect EB fluorescence. The flow rate was maintained at less than 300 cells per second. Clumps and doublets were excluded from analysis by electronic gating. Cell cycle phase compositions were determined using electronic gating as demonstrated in Fig. 3. Sub-G_0/G_1 cells were assumed to be apoptotic debris and excluded from the analysis. Samples were protected from light throughout the experiment. *In vitro* spectrofluorometry studies with isolated nuclei demonstrated no direct effects of MeHg on dye fluorescence properties (unpublished observations).

Cytotoxicity assay. Cells treated with final concentrations of 2, 4, and 6 μM MeHg for 24 h were assessed for cell viability using a lactate dehydrogenase (LDH) release assay (Boehringer Mannheim, Indianapolis, IN). Cell death was quantified by measuring the activity of LDH released into the culture supernatant from the cytosol of damaged cells. Briefly, 50 μl culture super-

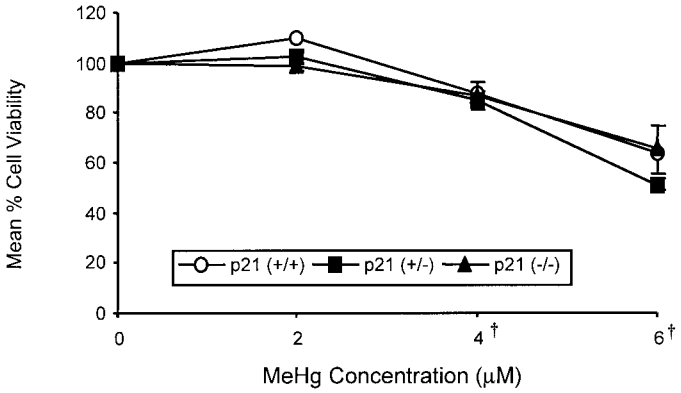

FIG. 1. Dose—response of primary MEFs of different p21 genotypes with MeHg treatment. Cultures (passages 4–6) of the indicated genotypes were treated with 0, 2, 4, and 6 μM MeHg for 24 h. Cytotoxicity was quantified using an LDH assay. Data ($n = 6$) are presented as mean percentage cell viability ± SE. †Means significantly different ($p \leq 0.05$ from the negative control. No significant difference in toxicity was observed between p21 genotypes.

natant from each treatment group was aliquoted into separate wells of a 96-well flat-bottom microtiter plate (Falcon, Lincoln Park, NJ). The volume in each well was brought up to 100 μl with sterile water and incubated with 100 μl of the reaction mixture containing diaphorase, NAD^+, sodium lactate, and tetrazolium salt INT (2-[4-iodophenyl]-3-[4-nitrophenyl]-5-phenyltetrazolium chloride) for 15 min, protected from light. Untreated cells were used as control for spontaneous LDH release. Maximum LDH release was estimated by measuring the LDH activity in the supernatant of untreated cells lysed with 2% Triton X-100 in culture media. The colorimetric reaction was quantified spectrophotometrically at 490 nm, using 690 nm as reference wavelength, in a microplate reader (Molecular Devices Corp., Palo Alto, CA). Spontaneous cell death was assumed to be minimal relative to cytotoxicity induced by MeHg. The percentage cell viability was calculated by subtracting percentage cytotoxicity from 100%.

Statistical analysis. Analysis of variance (ANOVA) was performed using the General Linear Model (GLM) General Factorial procedure. Dose and genotype were treated as factors while the measured endpoint was designated as the dependent variable. Duncan's multiple range test was used to evaluate the difference between specific means. A p value ≤ 0.05 was considered statistically significant. All statistical analyses were performed using SPSS for Windows Release 8.0.0 (SPSS Inc., Chicago, IL).

RESULTS

Dose-dependent MeHg-induced cytotoxicity. Primary mouse embryonic fibroblasts (MEFs) plated at passages 4–6 were treated with 2, 4, or 6 μM MeHg for 24 h. Cell death induced by MeHg was estimated by measuring the activity of the LDH released into the cell culture media (Fig. 1). We observed a concentration-dependent decrease in cell viability in all p21 genotypes after MeHg treatment. The decrease in the cell viability upon exposure to 4 or 6 μM MeHg was statistically significant ($p \leq 0.05$) compared to the negative (untreated) control as determined by ANOVA (General Factorial) and Duncan's multiple range test analyses. MeHg-induced toxicity did not differ across the p21 genotypes.

MeHg induced a p21-independent increase in G_2/M-phase population. p21 transgenic embryonic fibroblasts (passages 4–6) were treated with 2, 4, or 6 μM MeHg for 24 h and the distribution of cells in different phases of the cell cycle (i.e., G_0/G_1, S, and G_2/M) was analyzed by DNA content-based flow cytometry. Cells treated with 50 nM colchicine or sterile water were used as positive and negative controls, respectively. Analysis was conducted by comparing the average fraction of cells in each cell cycle phase as a function of MeHg concentration and p21 genotype (Fig. 2).

A statistically significant increase ($p \leq 0.05$) in the proportion of G_2/M-phase cells was observed upon treatment with 2 or 4 μM MeHg. The proportion of G_2/M-phase cells increased from 26.2 ± 2.6% without treatment to 36.0 ± 3.7% following exposure of p21(+/+) cultures to 2 μM MeHg for 24 h. The proportion of G_2/M-phase cells exhibited a comparable increase from 24.8 ± 2.6 to 35.1 ± 3.4% in p21(+/−) cultures, and 28.4 ± 1.7 to 41.5 ± 3.5% in p21(−/−) cultures, after treatment with 2 μM MeHg for 24 h. These increases in the proportion of G_2/M phase in response to MeHg were not statistically different between the p21 genotypes. Whereas the proportion of G_2/M-phase cells increased relative to controls following exposure to 2 or 4 μM MeHg, cells exposed to 6 μM MeHg for 24 h did not show a significant increase in the proportion of G_2/M-phase cells compared to controls in any p21 genotype.

As the fraction of the G_2/M cell population increased upon treatment with 2 or 4 μM MeHg, we observed a concomitant decrease in both G_0/G_1- and S-phase fractions. After 24 h of BrdU labeling, untreated p21(+/+) cells had 58.5 ± 3.2% in the G_0/G_1 phase and 15.2 ± 1.1% in the S phase. After treatment with 2 μM MeHg for 24 h, the fraction of p21(+/+) cells in G_0/G_1 decreased to 52.8 ± 4.4% and the S-phase population decreased to 11.2 ± 0.8%. Similar trends were observed upon MeHg exposure of p21(+/−) and p21(−/−) cells. As expected, cultures exposed to 50 nM colchicine accumulated in G_2/M within 24 h of exposure, consistent with the known inhibitory effects of colchicine on the mitotic spin-

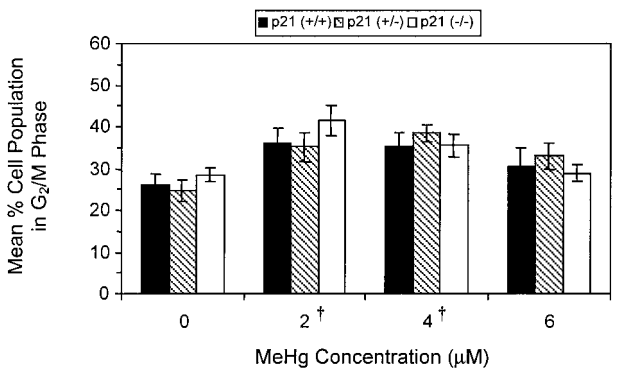

FIG. 2. Effect of MeHg on the G_2/M-phase population of primary MEFs of different p21 genotypes. Cultures (passages 4–6) of the indicated genotypes were treated with 0, 2, 4, and 6 μM MeHg for 24 h. Cells were harvested and analyzed based on DNA content using DAPI by flow cytometry ($n \geq 5$). †MeHg treatment groups significantly different ($p \leq 5$) relative to negative control (untreated cells). No significant difference in the proportion of G2/M-phase cells was observed between p21 genotypes.

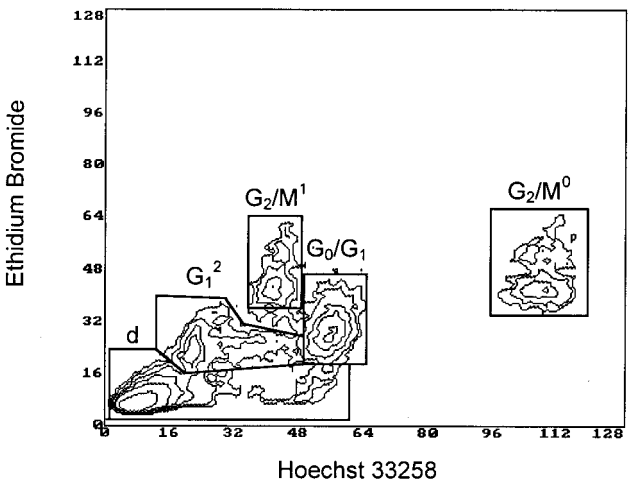

FIG. 3. Example of electronic gating used in flow cytometric bivariate analysis of MEFs stained with Hoechst 33258 and ethidium bromide after continuous labeling with BrdU. Cells in various cell cycle phases are labeled as follows: G_0/G_1, cells remaining in G_0/G_1 over the BrdU labeling period; G_2/M^0, cells remaining in G_2/M throughout the BrdU labeling period; G_2/M^1, cells reaching G_2/M from G_1 over the labeling period; and G_1^2, cells completing one round of cell proliferation over the BrdU labeling period. d, cell debris. Gating and data analysis were performed using the MPLUS cell cycle analysis software.

dle. The proportion of G_2/M-phase cells following exposure to 50 nM colchicine was comparable to that observed with either 2 or 4 μM MeHg.

MeHg inhibited cell cycle progression partially dependent on p21. To further evaluate the effects of MeHg on cell cycling, we performed bivariate BrdU–Hoechst flow cytometric analysis. The BrdU–Hoechst quenching method allows for monitoring of the proliferative history of cells over multiple rounds of cell proliferation. This ability to examine the proliferative history of specific cells arises from both the continuous BrdU labeling, which leads to BrdU accumulation in DNA in proportion to the number of rounds of DNA synthesis that have occurred during the labeling period, and from the observation that DNA regions where thymidine has been substituted by BrdU cannot be labeled by the bisbenzimidazole dyes Hoechst 33342 or 33258 (Bohmer, 1978; Kubbies and Friedl, 1985). Because BrdU for thymidine substitution occurs during DNA synthesis, there is a stoichiometric ''quenching'' effect on Hoechst fluorescence proportional to the amount of BrdU incorporated into newly synthesized DNA (Kubbies and Friedl, 1985; Latt *et al.,* 1977).

Asynchronous primary embryonic fibroblasts transgenic to p21 were exposed continuously to 90 μM BrdU and 2, 4, or 6 μM MeHg for up to 48 h to allow completion of at least one cell cycle. An example flow cytogram demonstrating the electronic gating used in the bivariate BrdU–Hoechst analysis is presented as Fig. 3. Representative flow cytograms of bivariate BrdU–Hoechst analysis of MeHg-treated p21(+/+) and p21(−/−) MEFs are presented in Fig. 4; cytograms of cultures treated with 2 μM MeHg were similar to the negative control and are therefore not shown. Because Hoechst staining is inversely proportional to BrdU incorporation, cells in G_2/M will have the highest Hoechst fluorescence; these cells are labeled G_2/M^0 in Figs. 3 and 4. Cells remaining in G_0/G_1 during the BrdU labeling period are labeled G_0/G_1, and untreated p21(+/+) and p21(−/−) cells that were able to complete one cell cycle during the BrdU labeling period are labeled G_1^2 in Figs. 3 and 4.

Figure 3 demonstrates the electronic gating used to evaluate the EBUS Hoechst 33258 bivariate flow cytograms. Inspection of the BrdU–Hoechst cytograms revealed some differences in cell proliferation and response to MeHg exposure across p21 genotypes. For example, compared to untreated controls (Figs. 4A and 4D), treatment of p21(+/+) cells with either 4 or 6 μM MeHg for 24 h (Figs. 4B and 4C, respectively) or treatment of p21(−/−) cells with 6 μM MeHg for 24 h (Fig. 4F) inhibited cell cycle progression in all cell cycle phases. This cell cycle block was demonstrated by the lack of S-, G_2/M^1-, and G_1^2-phase cells and the persistence of cells in G_2/M^0. Compared to untreated controls (Fig. 3D), the reduced appearance of G_1^2-phase cells following treatment of p21(−/−) cells with 4 μM MeHg suggests a reduction, but not a block, in cell cycle progression (Fig. 4E).

During 48 h of culture, untreated p21(+/+) and p21(−/−) cells continued cell cycling and reached G_2/M^2 (Figs. 4G and 4J, respectively). The accumulation of p21(−/−) and p21(+/+) cells in G_2/M^1 at 48 h suggests persistent mitotic inhibition by exposure to 4 μM MeHg (Figs. 4H and 4K, respectively). Whereas p21(−/−) cells treated with 6 μM MeHg for 48 h were able to proceed to G_2/M^1 (Fig. 4L), p21(+/+) cells remained blocked in all cell cycle phases and were not able to progress through the cell cycle (Fig. 4I).

Quantitative analysis of cell cycle progression was assessed by estimating the fraction of cells completing one cell cycle during the culture period and reaching G_1^2 (Fig. 5). As shown, MeHg induced a dose-dependent inhibition of cell cycle progression at both 4 and 6 μM after 24 and 48 h in all genotypes ($p \leq 0.05$). After 2 μM MeHg treatment for 48 h, a higher fraction (12.9 ± 2.0%) of p21(−/−) cells was able to reach G_1^2 compared to the p21(+/+) cells (6.0 ± 2.2%). This difference in ability to complete one round of cell division may be attributed to defective checkpoint control in the p21(−/−) cells (e.g., Deng *et al.,* 1995). Statistical analysis ($p \leq 0.05$) of the G_1^2 accumulation of p21(−/−) cells relative to doses of MeHg after 24 and 48 h demonstrated a significantly different response compared to the p21(+/+) and p21(+/−) cells.

Cells remaining in G_0/G_1 did not show a significant change in proportions upon MeHg treatment, however, the percentage of cells in G_0/G_1 significantly differed among the p21 genotypes. For example, 32.0 ± 7.0% of p21(+/+) cells were in G_0/G_1 at baseline (24 h) compared to 19.9 ± 10.2% of p21(+/−) cells and 42.2 ± 7.4% of p21(−/−) cells. A similar pattern was seen after 48 h, although the proportion of cells in

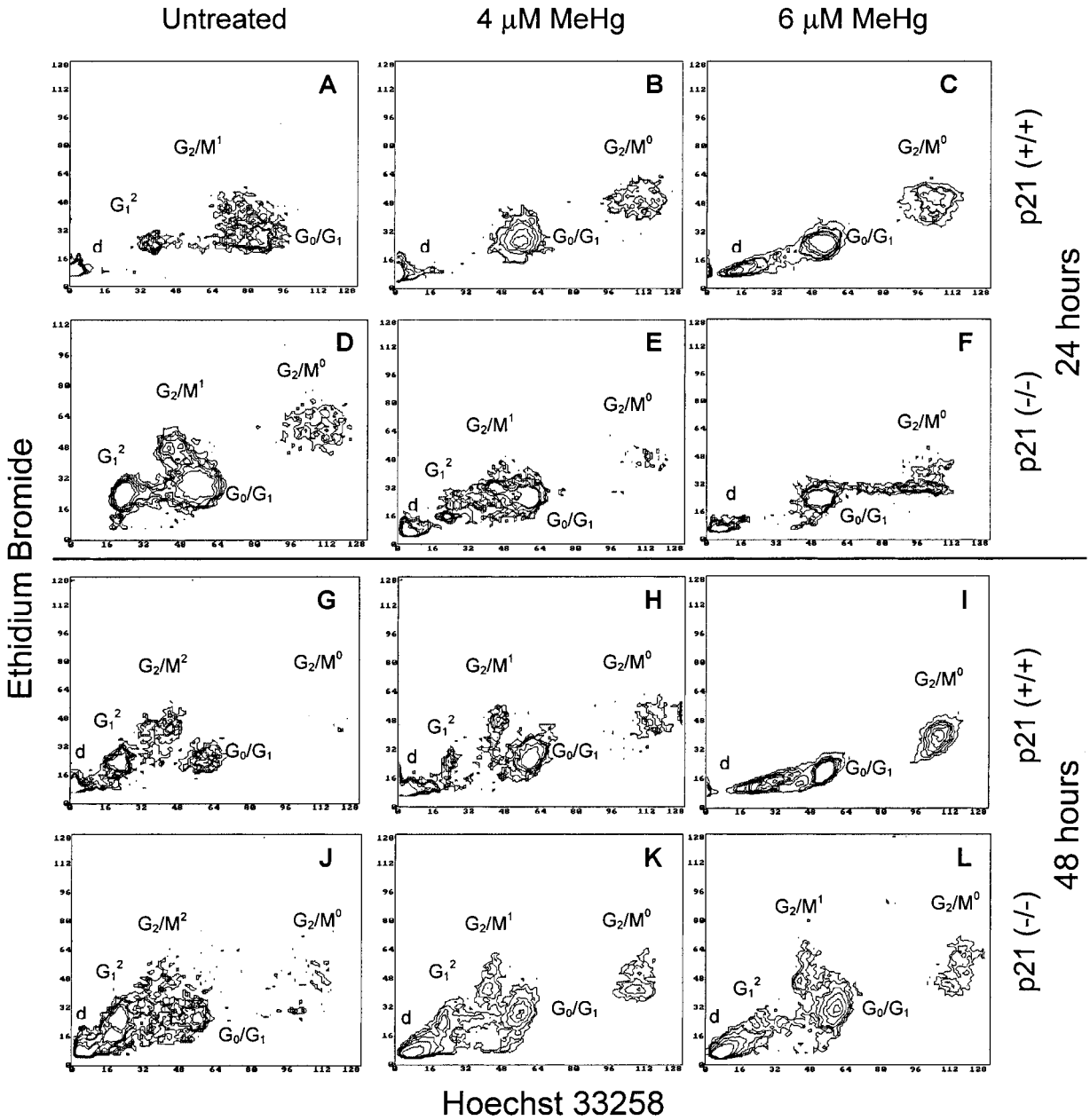

FIG. 4. Bivariate Hoechst vs ethidium bromide flow cytograms of MeHg-treated MEFs of different p21 genotypes. Asynchronous MEFs (passages 4–6) were treated with 0, 4, or 6 μM MeHg and continuously labeled with BrdU for 24 or 48 h. Cells were harvested and stained with Hoechst 33258 and ethidium bromide. Representative cytograms of p21(+/+) after 24 (A—C) and 48 h (G—I) of treatment are presented. p21(−/−) MEFs treated for 24 (D—F) and 48 h (J—L) are also shown. Cells in various cell cycle phases are labeled as follows: G_0/G_1, cells remaining in G_0/G_1 over the BrdU labeling period; G_2/M^0, cells remaining in G_2/M throughout the BrdU labeling period; G_2/M^1, cells reaching G_2/M from G_1 over the labeling period; and G_1^2, cells completing one round of cell proliferation over the BrdU labeling period; G_2/M^2, cells reaching G_2/M after completing one round of cell proliferation over the BrdU labeling period. d, cell debris.

G_0/G_1 decreased in all p21 genotypes, indicating that some fraction of the cells started cycling between 24 and 48 h.

DISCUSSION

Gene products such as p21[WAF1/CIP1] that function as cell cycle checkpoints maintain cellular integrity and ensure the proper completion of each stage in cell cycle progression necessary for normal growth (Shackelford *et al.*, 1999). In the present study, we used a transgenic *in vitro* system to evaluate the effect of partial (+/−) and complete (−/−) loss of p21, relative to the wild type (+/+) genotype, on the cell cycling inhibition induced by MeHg.

The kinase inhibitor p21 functions as a G_2 checkpoint by

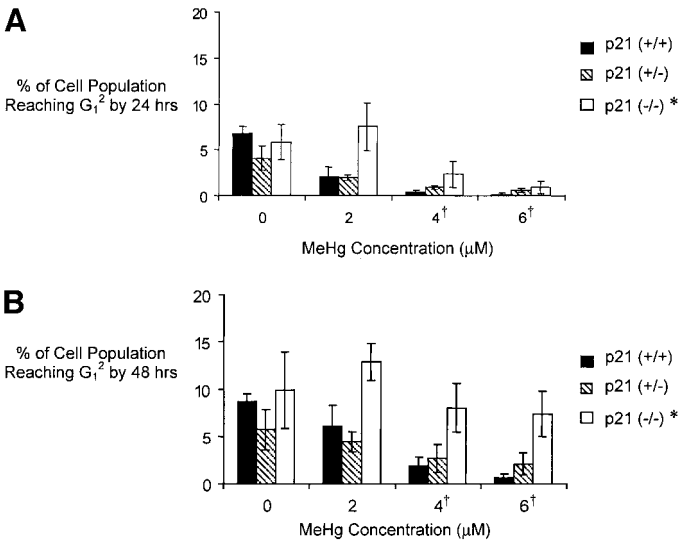

FIG. 5. Effect of MeHg on cell cycle progression of MEFs of different p21 genotypes. Asynchronous cells (passages 4–6) were treated with 0, 2, 4, and 6 μM MeHg and labeled with BrdU for 24 (A) and 48 h (B). Cells were harvested and then stained with Hoechst 33258 and ethidium bromide. The fraction of cells ($n \geq 3$) reaching second round G_1 (G_1^2) after 24 and 48 h or MeHg treatment is shown (mean ± SE). †Statistically significant differences ($p \leq 0.05$) relative to control untreated cells were observed across MeHg exposure groups. *Statistically significant differences ($p \leq 0.05$) relative to control untreated cells were observed across p21 genotype status.

binding to cyclin B1–cdc2 complexes, which are integral in the G_2/M transition (Barboule *et al.*, 1999; Dulic *et al.*, 1998). Binding of p21 to PCNA has also been reported to result in G_2 arrest (Cayrol *et al.*, 1998). Ponce *et al.* (1994) have previously shown G_2/M inhibition after exposure of primary rat fetal CNS cells to MeHg. Our results were consistent with this previous study and we further show that the G_2/M accumulation induced by MeHg was independent of p21 (Fig. 2). An increase in the proportion of cells in G_2/M was observed at 2 and 4 μM MeHg treatment ($p \leq 0.05$), but there was no difference among the p21 genotypes within each treatment group. Although MeHg exposures of 2 or 4 μM inhibited cell cycling in G_2/M, there was no significant change relative to untreated controls in the percentage of G_2/M-phase cells upon exposure to 6 μM MeHg in any p21 genotype (Fig. 2). The observed G_2/M-phase inhibition by 2 and 4 μM, but not 6 μM MeHg may be explained by the observed cell cycle inhibition across all cell cycle phases upon exposure to 6 μM MeHg (Fig. 4) and suggest that cell cycle control may be overwhelmed at 6 μM and cell death is favored. Complete inhibition of all cell cycling has been observed in primary rat neuroepithelial cell cultures exposed to 4 μM for 24 h (Ponce *et al.*, 1994) and in murine erythroleukemic cells exposed to 10 μM MeHg for 6 h (Zucker *et al.*, 1990).

Results from BrdU–Hoechst analyses suggest that p21 is partially involved in the observed MeHg inhibition of cell cycle progression (Figs. 4 and 5). In contrast, DAPI analyses suggest that the G_2/M accumulation induced by MeHg is not dependent on p21 status (Fig. 2). These results suggest a complex relationship between p21 and other cell cycle regulators in the control of cell proliferation following exposure to MeHg. Passage through G_1 has been previously shown to be prevented by p21 through inhibition of cyclin E–CDK2 complexes (Stewart *et al.*, 1999). In our study, we observed a higher fraction of p21(−/−) cells reaching the second round G_1 (termed G_1^2 in Fig. 4) compared to both p21(+/+) and p21(+/−) cells (Fig. 5). This may be attributed to the partial loss of the cell cycle checkpoint control in p21(−/−) cells resulting in a higher rate of progression through the cell cycle (Deng *et al.*, 1995) and greater leakage through cell cycle checkpoints. We did not observe a complete abrogation of the G_1 or G_2 checkpoints in the MeHg response of p21(−/−) cells; this may be due to possible involvement of other redundant pathways that ensure proper G_1 control such as those mediated by p16 and p27 (Shackelford *et al.*, 1999).

Transition from one cell cycle phase to another is controlled by CDKs and is regulated by the interaction of these kinases with various cyclins and specific inhibitors, and by intracellular localization. $p21^{WAF/CIP1}$ belongs to the Cip family of kinase inhibitors (Sherr, 1995). Cell cycle control by CDK inhibitors and cyclins depends on the protein content in each cell cycle phase, which is regulated by both transcription and proteolysis. Proteolysis involves an ATP-dependent activation of ubiquitin by a ubiquitin-activating enzyme (E_1 enzyme), formation of an E_1–ubiquitin thiol ester, and transfer of ubiquitin to the protein selected for degradation (Udvardy, 1996). The 26-kDa proteosome involved in this cell cycle proteolysis has been shown to be dependent on Ca^{2+} (Santella *et al.*, 1998). MeHg has been found to decrease intracellular ATP and to elevate intracellular calcium levels (Kauppinen *et al.*, 1989; Sarafian and Verity, 1993). One focus of our study has been on the effect of MeHg on transcription of cell cycle-related genes. Proteolysis is another pathway of cell cycle regulation by which MeHg may exert its effects on cell cycle inhibition.

The CDKs, a well-conserved family of serine/threonine protein kinases, exert control over the cell cycle through regulated protein phosphorylation (Arellano and Moreno, 1997). MeHg has been shown to affect protein phosphorylation (Kawamata *et al.*, 1987; Sarafian and Verity, 1990a, b, 1993; Yagame *et al.*, 1994) and kinase activity (Sarafian and Verity, 1993). MeHg has also been shown to have a high affinity for protein sulfhydryl groups (Hughes, 1957), which play a role in disulfide bond formation crucial in stabilizing the protein tertiary structure. Hence, MeHg effects on protein phosphorylation and protein stability are likely modes of MeHg interference in normal cell cycling. MeHg may cause DNA damage resulting in strand breaks (Betti *et al.*, 1993; Costa *et al.*, 1991), though its cytotoxicity likely limits its potency as a carcinogen or mutagen.

Results from the present work demonstrate a concentration- and time-dependent G_0/G_1 and G_2/M inhibition induced by MeHg in MEFs. Vogel *et al.* (1986) reported a similar finding

in normal human fibroblasts, where they observed a prolonged G_1 after exposure to 3 μM MeHg for 21 h and a G_2/M arrest after longer exposure. We have shown a similar increase in the G_2/M proportion after treatment with 2 and 4 μM MeHg and 50 nM colchicine in all p21 genotypes. This suggests spindle disturbance, which is a known mechanism of action of colchicine, as a possible pathway for MeHg-induced mitotic dysfunction (Miura *et al.*, 1978; Ponce *et al.*, 1994; Rodier *et al.*, 1984; Wasteneys *et al.*, 1988). MeHg binding to cysteine residues of tubulin has been suggested to block microtubule assembly (Sager and Syversen, 1986). Because MeHg binds to tubulin dimers at stoichiometric ratios (Vogel *et al.*, 1985), it is possible that, at low concentrations of MeHg, some microtubules are still able to assemble into a functional mitotic apparatus and, thus, some fraction of cells are still able to cycle. Vogel *et al.* (1985) have previously reported that polymerization of crude rat microtubules exposed to 1 μM MeHg are only 4% inhibited. There were less pronounced MeHg effects on p21 transgenic MEFs in G_0/G_1, than G_2/M, which may be due to higher sensitivity of microtubules in dividing cells than interphase microtubules (Wasteneys *et al.*, 1988).

In addition to direct tubulin depolymerization, MeHg may alter tubulin polymerization status indirectly through mitochondrial dysfunction, resulting in low intracellular ATP and, possibly, elevated intracellular calcium levels (Kauppinen *et al.*, 1989). Decreased ATP levels may affect spindle elongation during anaphase and microtubule assembly, which requires GTP (Onfelt, 1986). Intracellular levels of calcium may modulate microtubule polymerization and stability through direct association with tubulin and via calcium-dependent phosphorylation of microtubule-associated proteins (Nicotera *et al.*, 1992; Onfelt, 1986). Thus, MeHg may exert both direct and indirect effects on the spindle apparatus important in the cell cycle machinery.

Our estimation of the fraction of cells completing one round of cell division required judgment about where to set the electronic gates (as shown in Fig. 3). This gating was particularly challenging because of the relatively broad coefficient of variation of cells in any given phase of the cell cycle along both the Hoechst and ethidum bromide axes, which is an inherent difficulty of this type of analysis with fibroblastic cells. The electronic gating was conducted so as to split the troughs between concentrations of cells and used the G_0/G_1 and G_2/M^0 peaks to anchor the analysis of G_1^2 and G_2/M^1 cells. It is likely that there was some spillover of S-phase cells into the G_2/M^1 population and debris into the G_1^2 population. The effect of this contamination is difficult to estimate, but sensitivity analyses we conducted to examine the effect of minor variations in the electronic gating suggested no qualitatitve differences to the conclusions reached in this report and error in the population estimates of 10–15% or less.

We evaluated the effect of MeHg on cell viability using the LDH release assay to quantify cell death resulting from MeHg exposure. We chose a cell death assay instead of a live cell assay to circumvent possible confounding by the higher rate of cell proliferation in the null genotypes that may mask the true magnitude of cytotoxicity. The cytotoxicity observed at the experimental doses was relatively low compared to those observed in other previous studies (Ponce *et al.*, 1994; Sarafian and Verity, 1990a), which may be due to differential sensitivity of the cell systems and assay endpoint. Sager *et al.* (1984) have observed resistance of fibroblasts to MeHg-induced microtubule disruption compared to neuroblastoma cells exposed to similar concentrations. LDH is a cytoplasmic enzyme that is rapidly released into the cell culture supernatant upon damage to the plasma membrane. Cells undergoing apoptosis, especially during the early stages in which the cell membrane is still intact, may not be captured by the LDH release assay. Shenker *et al.* (1997) have reported that human T-cells exposed to 1–5 μM MeHgCl undergo apoptosis. Sane *et al.* (1999) have shown arrested cells in G_1 exit the cell cycle and proceed to cell death through necrosis. Therefore, the effect of MeHg on cell proliferation may be a combination of cell cycle inhibition and cell death. To further elucidate this, multiparameter flow cytometry may be employed combining apoptosis, necrosis, and DNA content-based cell cycle analysis.

Results from the present study support current knowledge about the mechanism of MeHg toxicity, particularly on cell cycle inhibition as a possible cause of decreased neuronal cell counts previously observed in the brains of infants and animals exposed to MeHg *in utero*. Our data also suggest other possible underlying factors contributing to cell cycle regulation in response to MeHg. The present work may also provide insights that will allow more accurate assessment of risk for specific subpopulations of individuals with particular genetic susceptibilities. *In vivo* studies, evaluation of other cell cycle proteins and regulation pathways, and cell death (apoptosis versus necrosis) experiments will provide additional information in the further understanding of the effects of MeHg on cell proliferation.

ACKNOWLEDGMENTS

The authors gratefully acknowledge support from the Center for Ecogenetics and Environmental Health at the University of Washington, Department of Environmental Health (NIH Grant 5 P30 ES 0733), the U.S. Environmental Protection Agency (R825358), and the National Institutes of Health (R01 ES10613–01).

REFERENCES

Arellano, M., and Moreno, S. (1997). Regulation of CDK/cyclin complexes during the cell cycle. *Int. J. Biochem. Cell. Biol.* **29,** 559–573.

Barboule, N., Lafon, C., Chadebech, P., Vidal, S., and Valette, A. (1999). Involvement of p21 in the PKC-induced regulation of the G2/M cell cycle transition. *FEBS Lett.* **444,** 32–37.

Betti, C., Barale, R., and Pool-Zobel, B. L. (1993). Comparative studies on cytotoxic and genotoxic effects of two organic mercury compounds in lymphocytes and gastric mucosa cells of Sprague–Dawley rats. *Environ. Mol. Mutagen* **22**(3), 172–180.

Bohmer, R. M. (1978). Cell kinetic analysis using a combination of the BrdU/33258 Hoechst technique with flow cytometry. In *Biomathematics and Cell Kinetics* (A. J. Valleron and P. D. Macdonald, Eds.), pp. 405–410. Elsevier, Amsterdam.

Bohmer, R. M. (1979). Flow cytometric cell cycle analysis using the quenching of 33258 Hoechst fluorescence by bromodeoxyuridine incorporation. *Cell Tissue Kinet.* **12,** 101–110.

Bohmer, R. M., and Ellwart, J. (1981). Combination of BrdU-quenched Hoechst fluorescence with DNA-specific ethidium bromide fluorescence for cell cycle analysis with a two-parameter flow cytometer. *Cell Tissue Kinet.* **14,** 653–658.

Brugarolas, J., Moberg, K., Boyd, S. D., Taya, Y., Jacks, T., and Lees, J. A. (1999). Inhibition of cyclin-dependent kinase 2 by p21 is necessary for retinoblastoma protein-mediated G1 arrest after gamma-irradiation. *Proc. Natl. Acad. Sci. USA* **96,** 1002–1007.

Bunz, F., Dutriaux, A., Lengauer, C., Waldman, T., Zhou, S., Brown, J. P., Sedivy, J. M., Kinzler, K. W., and Vogelstein, B. (1998). Requirement for p53 and p21 to sustain G2 arrest after DNA damage. *Science* **282,** 1497–1501.

Cayrol, C., Knibiehler, M., and Ducommun, B. (1998). p21 binding to PCNA causes G1 and G2 cell cycle arrest in p53-deficient cells. *Oncogene* **16,** 311–320.

Choi, B. H. (1986). Methylmercury poisoning of the developing nervous system. I. Pattern of neuronal migration in the cerebral cortex. *Neurotoxicology* **7,** 591–600.

Choi, B. H. (1989). The effects of methylmercury on the developing brain. *Prog. Neurobiol.* **32,** 447–470.

Choi, B. H., Lapham, L. W., Amin-Zaki, L., and Saleem, T. (1978). Abnormal neuronal migration, deranged cerebral cortical organization, and diffuse white matter astrocytosis of human fetal brain: A major effect of methylmercury poisoning in utero. *J. Neuropathol. Exp. Neurol.* **37,** 719–733.

Costa, M., Christie, N. T., Cantoni, O., Zelikoff, J. T., Wang, X. W., and Rossman, T. G. (1991). DNA damage by mercury compounds: An overview. In *Advances in Mercury Toxicology* (Suzuki, T., Ed.), pp. 255–273, Plenum Press, NY.

Cox, L. S. (1997). Multiple pathways control cell growth and transformation: Overlapping and independent activities of p53 and p21Cip1/WAF1/Sdi1. *J. Pathol.* **183,** 134–140.

Cox, L. S., and Lane, D. P. (1995). Tumour suppressors, kinases and clamps: How p53 regulates the cell cycle in response to DNA damage. *Bioessays* **17,** 501–508.

Deng, C., Zhang, P., Harper, J. W., Elledge, S. J., and Leder, P. (1995). Mice lacking p21CIP1/WAF1 undergo normal development, but are defective in G1 checkpoint control. *Cell* **82,** 675–684.

Dulic, V., Stein, G. H., Far, D. F., and Reed, S. I. (1998). Nuclear accumulation of p21Cip1 at the onset of mitosis: A role at the G2/M-phase transition. *Mol. Cell. Biol.* **18,** 546–557.

Eto, K., Oyanagi, S., Itai, Y., Tokunaga, H., Takizawa, Y., and Suda, I. (1992). A fetal type of Minamata disease. An autopsy case report with special reference to the nervous system. *Mol. Chem. Neuropathol.* **16,** 171–186.

Geelen, J. A., Dormans, J. A., and Verhoef, A. (1990). The early effects of methylmercury on the developing rat brain. *Acta Neuropathol.* **80,** 432–438.

Harada, M. (1978). Congenital Minamata disease: Intrauterine methylmercury poisoning. *Teratology* **18,** 285–288.

Harada, Y. (1977). Congenital Minamata disease. In *Minamata Disease: Methyl Mercury Poisoning in Minamata and Niigata* (R. Tsubak and K. Irukayama, Eds.), pp. 209–239. Kodansha, Tokyo.

Herschkowitz, N. (1988). Brain development in the fetus, neonate and infant. *Biol. Neonate* **54,** 1–19.

Howard, J. D., and Mottet, N. K. (1986). Effects of methylmercury on the morphogenesis of the rat cerebellum. *Teratology* **34,** 89–95.

Hughes, W. L. (1957). A physicochemical rationale for the biological activity of mercury and its compounds. *Ann. NY Acad. Sci.* **65,** 454–460.

Kauppinen, R. A., Komulainen, H., and Taipale, H. (1989). Cellular mechanisms underlying the increase in cytosolic free calcium concentration induced by methylmercury in cerebrocortical synaptosomes from guinea pig. *J. Pharmacol. Exp. Ther.* **248,** 1248–1254.

Kawamata, O., Kasama, H., Omata, S., and Sugano, H. (1987). Decrease in protein phosphorylation in central and peripheral nervous tissues of methylmercury-treated rat. *Arch. Toxicol.* **59,** 346–352.

Kubbies, M., and Friedl, R. (1985). Flow cytometric correlation between BrdU/Hoechst quench effect and base pair composition in mammalian cell nuclei. *Histochemistry* **83,** 133–137.

Latt, S. A., George, Y. S., and Gray, J. W. (1977). Flow cytometric analysis of bromodeoxyuridine-substituted cells stained with 33258 Hoechst. *J. Histochem. Cytochem.* **25,** 927–934.

Levitt, P., Reinoso, B., and Jones, L. (1998). The critical impact of early cellular environment on neuronal development. *Prev. Med.* **27,** 180–183.

Marsh, D. O., Myers, G. J., Clarkson, T. W., Amin-Zaki, L., Tikriti, S., and Majeed, M. A. (1980). Fetal methylmercury poisoning: Clinical and toxicological data on 29 cases. *Ann. Neurol.* **7,** 348–353.

Matsumoto, H., Koya, G., and Takeuchi, T. (1965). Fetal Minamata disease: A neuropathological study of two cases of intrauterine intoxication by a methyl mercury compound. *J. Neuropath. Exp. Neurol.* **24,** 563–574.

Miura, K., Suzuki, K., and Imura, N. (1978). Effects of methylmercury on mitotic mouse glioma cells. *Environ. Res.* **17,** 453–471.

Mottet, N. K. (1989). A pathologist's perspective on the toxic effects of mercury compounds. *Comments Toxicol.* **3,** 179–190.

Nicotera, P., Bellomo, G., and Orrenius, S. (1992). Calcium-mediated mechanisms in chemically induced cell death. *Annu. Rev. Pharmacol. Toxicol.* **32,** 449–470.

Niculescu III, A. B., Chen, X., Smeets, M., Hengst, L., Prives, C., and Reed, S. I. (1998). Effects of p21(Cip1/Waf1) at both the G1/S and the G2/M cell cycle transitions: PRb is a critical determinant in blocking DNA replication and in preventing endoreduplication [published erratum appears in *Mol. Cell. Biol.* 1998, **18,** 1763]. *Mol. Cell. Biol.* **18,** 629–643.

Onfelt, A. (1986). Mechanistic aspects on chemical induction of spindle disturbances and abnormal chromosome numbers. *Mutat. Res.* **168,** 249–300.

Ou, Y. C., Thompson, S. A., Ponce, R. A., Schroeder, J., Kavanagh, T. J., and Faustman, E. M. (1999). Induction of the cell cycle regulatory gene p21 (Waf1, Cip1) following methylmercury exposure *in vitro* and *in vivo*. *Toxicol. Appl. Pharmacol.* **157,** 203–212.

Ponce, R. A., Kavanagh, T. J., Mottet, N. K., Whittaker, S. G., and Faustman, E. M. (1994). Effects of methyl mercury on the cell cycle of primary rat CNS cells *in vitro*. *Toxicol. Appl. Pharmacol.* **127,** 83–90.

Poot, M., Hoehn, H., Kubbies, M., Grossmann, A., Chen, Y. C., and Rabinovitch, P. S. (1990). Cell cycle analysis using continuous bromodeoxyuridine labeling and Hoechst 33258–ethidium bromide bivariate flow cytometry. *Methods Cell Biol.* **33,** 185–198.

Rabinovitch, P. S. (1983). Regulation of human fibroblast growth rate by both noncycling cell fraction and transition probability is shown by growth in 5-bromodeoxyuridine followed by Hoechst 33258 flow cytometry. *Proc. Natl. Acad. Sci. USA* **80,** 2951–2955.

Rabinovitch, P. S., Kubbies, M., Chen, Y. C., Schindler, D., and Hoehn, H. (1988). BrdU–Hoechst flow cytometry: A unique tool for quantitative cell cycle analysis. *Exp. Cell Res.* **174,** 309–318.

Reid, B. J., Blount, P. L., Rubin, C. E., Levine, D. S., Haggitt, R. C., and Rabinovitch, P. S. (1992). Flow-cytometric and histological progression to malignancy in Barrett's esophagus: Prospective endoscopic surveillance of a cohort [see comments]. *Gastroenterology* **102,** 1212–1219.

Reid, B. J., Haggitt, R. C., Rubin, C. E., and Rabinovitch, P. S. (1987). Barrett's esophagus. Correlation between flow cytometry and histology in detection of patients at risk for adenocarcinoma. *Gastroenterology* **93,** 1–11.

Rigberg, D. A., Blinman, T. A., Kim, F. S., Cole, M. A., and McFadden, D. W. (1999). Antisense blockade of p21/WAF1 decreases radiation-induced G2 arrest in esophageal squamous cell carcinoma. *J. Surg. Res.* **81,** 6–10.

Robertson, E. J. (Ed.) (1987). Embryo-derived stem cell lines. *In* Teratocarcinomas and Embryonic Stem Cells: A Practical Approach, pp. 71–112, IRL Press, Oxford.

Rodier, P. M., Aschner, M., and Sager, P. R. (1984). Mitotic arrest in the developing CNS after prenatal exposure to methylmercury. *Neurobehav. Toxicol. Teratol.* **6,** 379–385.

Rodier, P. M., Ingram, J. L., Tisdale, B., Nelson, S., and Romano, J. (1996). Embryological origin for autism: Developmental anomalies of the cranial nerve motor nuclei. *J. Comp. Neurol.* **370,** 247–261.

Sager, P. R., Aschner, M., and Rodier, P. M. (1984). Persistent, differential alterations in developing cerebellar cortex of male and female mice after methylmercury exposure. *Brain Res.* **314,** 1–11.

Sager, P. R., and Syversen, L. M. (1986). Disruption of microtubles by methylmercury. In *The Cytoskeleton* (T. W. Clarkson, P. R. Sager, and T. L. M. Syversen, Eds.), pp. 97–116. Plenum, New York.

Sane, A. T., and Bertrand, R. (1999). Caspase inhibition in camptothecin-treated U-937 cells is coupled with a shift from apoptosis to transient G1 arrest followed by necrotic cell death. *Cancer Res.* **59**(15), 3565–3569.

Santella, L., Kyozuka, K., De Riso, L., and Carafoli, E. (1998). Calcium, protease action, and the regulation of the cell cycle. *Cell Calcium* **23,** 123–130.

Sarafian, T., and Verity, M. A. (1990a). Altered patterns of protein phosphorylation and synthesis caused by methyl mercury in cerebellar granule cell culture. *J. Neurochem.* **55,** 922–929.

Sarafian, T., and Verity, M. A. (1990b). Methyl mercury stimulates protein 32P phospholabeling in cerebellar granule cell culture. *J. Neurochem.* **55,** 913–921.

Sarafian, T. A., and Verity, M. A. (1993). Changes in protein phosphorylation in cultured neurons after exposure to methyl mercury. *Ann. NY Acad. Sci.* **679,** 65–77.

Shackelford, R. E., Kaufmann, W. K., and Paules, R. S. (1999). Cell cycle control, checkpoint mechanisms, and genotoxic stress. *Environ. Health Perspect.* **107**(Suppl. 1), 5–24.

Shenker, B. J., Datar, S., Mansfield, K., and Shapiro, I. M. (1997). Induction of apoptosis in human T-cells by organomercuric compounds: A flow cytometric analysis. *Toxicol. Appl. Pharmacol.* **143**(2), 397–406.

Sherr, C. J. (1995). Mammalian G1 cyclins and cell cycle progression. *Proc. Assoc. Am. Phys.* **107,** 181–186.

Stewart, Z. A., Leach, S. D., and Pietenpol, J. A. (1999). p21(Waf1/Cip1) inhibition of cyclin E/Cdk2 activity prevents endoreduplication after mitotic spindle disruption. *Mol. Cell. Biol.* **19,** 205–215.

Takeuchi, T. (1968). Pathology of Minamata disease. In *Minamata Disease*. Kumamoto University, Kumamoto, Japan.

Takeuchi, T. (1977). Pathology of fetal Minamata disease: The effect of methylmercury on human intrauterine life. *Pediatrics* **6,** 69–87.

Udvardy, A. (1996). The role of controlled proteolysis in cell-cycle regulation. *Eur. J. Biochem.* **240,** 307–313.

Vogel, D. G., Margolis, R. L., and Mottet, N. K. (1985). The effects of methyl mercury binding to microtubules. *Toxicol. Appl. Pharmacol.* **80,** 473–486.

Vogel, D. G., Rabinovitch, P. S., and Mottet, N. K. (1986). Methylmercury effects on cell cycle kinetics. *Cell Tissue Kinet.* **19,** 227–242.

Wasteneys, G. O., Cadrin, M., Reuhl, K. R., and Brown, D. L. (1988). The effects of methylmercury on the cytoskeleton of murine embryonal carcinoma cells. *Cell Biol. Toxicol.* **4,** 41–60.

Yagame, H., Horigome, T., Ichimura, T., Uchiyama, J., and Omata, S. (1994). Differential effects of methylmercury on the phosphorylation of protein species in the brain of acutely intoxicated rats. *Toxicology* **92,** 101–113.

Zucker, R. M., Elstein, K. H., Easterling, R. E., and Massaro, E. J. (1990). Flow cytometric analysis of the mechanism of methylmercury cytotoxicity. *Am. J. Pathol.* **137,** 1187–1198.